INFECTION AND IMMUNITY, Dec. 2003, p. 7087–7098 Vol. 71, No. 12
0019-9567/03/$08.00+0 DOI: 10.1128/IAI.71.12.7087–7098.2003
Copyright © 2003, American Society for Microbiology. All Rights Reserved.

Infection and Inflammation in Skeletal Muscle from Nonhuman Primates Infected with Different Genospecies of the Lyme Disease Spirochete *Borrelia burgdorferi*

Diego Cadavid,[1]* Yunhong Bai,[1] Donna Dail,[1] Marie Hurd,[1] Kavi Narayan,[1] Emir Hodzic,[2] Stephen W. Barthold,[2] and Andrew R. Pachner[1]

Department of Neuroscience, University of Medicine and Dentistry of New Jersey—New Jersey Medical School, Newark, New Jersey 07103,[1] and Center for Comparative Medicine, University of California at Davis, Davis, California 95616[2]

Received 17 June 2003/Returned for modification 31 July 2003/Accepted 2 September 2003

Lyme borreliosis is a multisystemic disease caused by various genospecies of the spirochete *Borrelia burgdorferi*. To investigate muscle involvement in the nonhuman primate (NHP) model of Lyme disease, 16 adult *Macaca mulatta* animals inoculated with strain N40 of *B. burgdorferi* sensu strictu by syringe or by tick bite or with strain Pbi of *B. burgdorferi* genospecies *garinii* by syringe were studied. Animals were necropsied while immunosuppressed on day 50 (two animals each inoculated with *B. burgdorferi* N40 by syringe and with *B. garinii* Pbi by syringe) or on day 90, 40 days after immunosuppression had been discontinued (four animals each inoculated with strain N40 by syringe, with strain N40 by tick bite, and with strain Pbi by syringe). Skeletal muscles removed at necropsy were studied by (i) microscopic examination of hematoxylin-eosin-stained sections for inflammation and tissue injury; (ii) immunohistochemical and digital image analyses for antibody and complement deposition and cellular inflammation; (iii) Western blot densitometry for the presence of antibodies; and (iv) reverse transcription-PCR for measurement of the spirochetal load or C1q (the first component of the complement cascade) synthesis. The results showed that N40 was more infectious for NHPs than Pbi. NHPs inoculated with N40 but not with Pbi developed myositis. The inflammation in skeletal muscle was more severe in NHPs inoculated with N40 by syringe than in those inoculated by tick bite. The predominant cells in the inflammatory infiltrate were T cells and plasma cells. The deposition of antibody and complement in inflamed muscles from N40-inoculated NHPs was significantly higher than that in Pbi-inoculated NHPs. The spirochetal load was very high in the two N40-inoculated NHPs examined while they were immunosuppressed but decreased to minimal levels in the NHPs when immunocompetence was restored. We conclude that myositis can be a prominent feature of Lyme borreliosis depending on the infecting organism and host immune status.

Lyme borreliosis is a systemic disease caused by infection with the spirochete *Borrelia burgdorferi* (10). It is presently the most common arthropod-borne disease in the United States, where thousands of cases are reported to the Centers for Disease Control and Prevention every year (15). At least three genospecies pathogenic to humans have been characterized: *B. burgdorferi* sensu stricto, *B. afzelii*, and *B. garinii*. Only *B. burgdorferi* sensu stricto is endemic in North America, while all three genospecies are endemic in Europe. The organs most often affected are the skin, the joints, the heart, and the central and peripheral nervous systems (56). Neurological manifestations of *B. burgdorferi* infection, known as Lyme neuroborreliosis, occur in 5 to 20% of patients in North America (23, 60). They include aseptic meningitis, facial nerve palsy, radiculitis, peripheral neuropathy, myositis, and encephalopathy (39).

Myositis has been reported as a complication of Lyme borreliosis in both the United States (2) and Europe (28). In one series from the United States, 40% of 312 patients with Lyme borreliosis had myalgia and 4% had muscle tenderness (57). Myositis is also a feature of several animal models of Lyme borreliosis (36, 49). The pathogenesis of Lyme borreliosis has been studied with nonhuman primates (NHPs) inoculated by syringe with North American sensu stricto strain N40 of *B. burgdorferi* (42). During infections of immunosuppressed NHPs inoculated by syringe with N40, we found that skeletal muscles had the highest spirochetal load of all the tissues examined (11). During infections of transiently immunosuppressed (TISP) NHPs, we found that skeletal and cardiac muscles had the most severe inflammation of all the tissues examined (40).

The goal of the present study was to continue the characterization of skeletal muscle involvement in Lyme borreliosis in primates. Specifically, we compared the effects of infection with different genospecies of *B. burgdorferi* on skeletal muscle involvement, (ii) compared the effects of tick bite versus needle inoculation with strain N40, and (iii) studied the inflammatory responses in skeletal muscles at the cellular and molecular levels.

MATERIALS AND METHODS

Animals and *Borrelia* strains. Sixteen male adult *Macaca mulatta* animals with an average age of 3.5 years (range, 3 to 4) were inoculated for these experiments. Tissues from two additional *M. mulatta* animals that were never inoculated with borreliae were used as negative controls. The housing and care were in accordance with the Animal Welfare Act and the *Guide for the Care and Use of Laboratory Animals* in facilities accredited by the American Association for

* Corresponding author. Mailing address: UMDNJ—New Jersey Medical School, Department of Neuroscience, 185 South Orange Ave., MSB H506, Newark, NJ 07103. Phone: (973) 972-8686. Fax: (973) 972-5059. E-mail: Cadavidi@umdnj.edu.

TABLE 1. Infection, immunity, and inflammation in NHPs inoculated with borreliae[a]

NHP no.	Strain	Inoculation	Immunosuppression	Day of necropsy	Anti-*B. burgdorferi* immunoglobulin[b]	Infection[c]	Myositis[d]
794	N40	Needle	IC	120	+	None	−
793			IC	120	+	None	−
099			TISP	90	+	Minimal	+
177			TISP	90	+	Minimal	+
199			TISP	90	+	Minimal	+
383			TISP	90	+	Minimal	+
794			IS	50	+	High	+
372			IS	50	+	High	−
154	N40	Tick bite	TISP	90	+	Minimal	+
192			TISP	90	+	Minimal	+
211			TISP	90	+	Minimal	+
242			TISP	90	+	Minimal	+
321	Pbi	Needle	TISP	90	±[e]	None	−
105			TISP	90	+	None	−
012			TISP	90	−	None	−
981			TISP	90	−	None	−

[a] NHPs that were IC, TISP, or IS were examined by necropsy 50 to 120 days after intradermal inoculation with *B. burgdorferi* sensu stricto strain N4O or *B. garinii* strain Pbi.
[b] As determined by ELISA with whole-cell sonicates.
[c] As determined by TaqMan RT-PCR amplification of the 16S rRNA of *Borrelia* spp. with 1 μg of skeletal muscle RNA as a template.
[d] As determined by microscopic examination of HE-stained sections.
[e] Positive only when sera were diluted ≤1:500 (as opposed to the standard 1:5,000 dilution).

Accreditation of Laboratory Animal Care. All inoculations were done intradermally with strain N40 of *B. burgdoferi* sensu stricto by needle ($n = 8$) or by tick bite ($n = 4$) or with strain Pbi of *B. garinii* by needle ($n = 4$). For needle inoculation, a total dose of 10^6 spirochetes was injected intradermally over 8 to 10 different areas of shaved skin on the backs of the animals.

Tick inoculation. *Ixodes scapularis* ticks free of *B. burgdorferi* inherited infection were obtained as field-collected adults from southern Connecticut (cordially provided by Durland Fish, Yale University, New Haven, Conn.). A single cohort of adult ticks produced all of the larvae used for the tick-inoculation experiments described in this study. To generate infected nymphs, larvae were allowed to engorge on C3H mice that had been infected with *B. burgdorferi* for 2 weeks. Engorged larvae were collected and then allowed to molt and harden into nymphs. Ten percent of the pool of molted infected nymphs was tested by real-time PCR. The results showed that 97.3% were PCR positive for *B. burgdorferi* DNA. The average number of spirochetes per nymph was 4.15×10^4 (standard deviation [SD], $\pm 3.2 \times 10^4$). Prior to tick infestation (day 3), NHPs were habituated to a vest. On day 0, the skin between the shoulders was shaved, a tick chamber was placed on that area, and then eight infected nymphal ticks were placed in the chamber for each monkey. The chambers were inspected on days 1, 2, and 3 to assess the number of attached ticks. If fewer than four ticks were attached, three additional ticks were introduced for each unfed tick. The number of engorged nymphs per animal was in the range of five to eight. All of the ticks were collected from each animal and tested by real-time PCR. The results showed that all of them were PCR positive, with an average number of spirochetes per nymph of 3.5×10^5 (SD, $\pm 2.11 \times 10^5$).

Borreliae were cultured at 34°C in BSK-H medium with 6% rabbit serum (Sigma). All but two NHPs were immunosuppressed with dexamethasone starting 1 week prior to inoculation (day −7) (Table 1 and Fig. 1). The duration of immunosuppression varied: 10 NHPs were TISP, and 4 were permanently immunosuppressed (IS) (Fig. 1). Blood and cerebrospinal fluid were collected every 2 to 3 weeks to test for the presence of anti-*B. burgdorferi* antibodies. IS and TISP NHPs were euthanatized 50 and 90 days after inoculation, respectively. Immunocompetent (IC) NHPs were euthanatized 4 months after inoculation. After exanguination and intracardiac perfusion with buffer to minimize blood contamination, several tissues were collected (11). Tissues were processed by routine formalin fixation and embedding in paraffin or snap-frozen in isopentane chilled to less than −140°C in liquid nitrogen. Paraffin sections were cut at 5 μm, and frozen sections were cut at 8 μm.

HE staining. Inflammation was assessed by examination with hematoxylin-eosin (HE) staining. To compare the severity of inflammation, HE-stained muscle sections were scored by a masked examiner (D.C.) on the basis of the mean number of inflammatory foci per ×40 microscopic field as follows: no inflammation, 0; 1 to 3 foci, 1+; 4 to 10 foci, 2+; 11 to 20 foci, 3+; and more than 20 foci, 4+.

ELISA. A serum enzyme-linked immunosorbent assay (ELISA) was performed as described previously (43) with some modifications. Each plate contained a positive control. The antigens were sonicates of *B. burgdorferi* strains N40 and Pbi (9). Two hundred microliters of sonicate coating solution was added to microtitration plates (Linbro Scientific, Hamden, Conn.) at a concentration of 5 μg/ml and incubated overnight at 4°C (43). The plates were washed three times with phosphate-buffered saline (PBS)–0.05% Tween 20, and 200 μl of monkey sera was added at a 1:5,000 dilution. Sera found to be negative were run again at lower dilutions, as low as 1:200. The plates were incubated with primary antibody for 2 h at 37°C and washed again as described above. Two hundred microliters of horseradish peroxidase-conjugated donkey anti-human immunoglobin G (IgG) or IgM (Jackson Immunoresearch) was diluted 1:10,000 in PBS-Tween 20 and added to each well, and incubation was continued for an additional 2 h at 37°C. The plates were washed, and 200 μl of tetramethylbenzidine chromogen was added to each well, followed after 5 to 10 min by 50 μl of 8% sulfuric acid

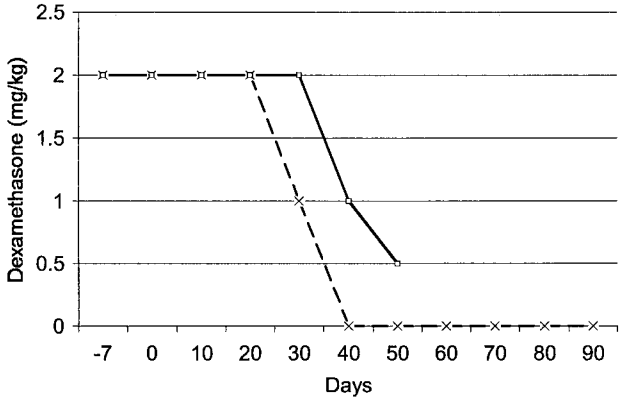

FIG. 1. Immunosuppression of the majority of NHPs with dexamethasone to increase the probability of infection, starting 1 week prior to inoculation. Some NHPs were necropsied 40 days after discontinuation of dexamethasone (TISP; broken line). Others were necropsied while still receiving dexamethasone (IS; solid line).

to stop the reaction. The plates were read immediately with an ELISA spectrophotometer (Bio-Rad). The standard positive control was serum obtained from a monkey with high titers of IgG and IgM antibodies and run within its linear range of dilutions. All serum samples were tested in duplicate.

Immunohistochemical and digital image analyses. Immunohistochemical analysis was performed as previously described (11, 12). Endogenous peroxidase activity was reduced by incubation with 3% H_2O_2 for 10 min at room temperature. Nonspecific binding was blocked with 3% normal monkey serum for frozen sections or Power Block (Biogenex) for paraffin sections. Rabbit anti-human IgG (Dako A0423), IgM (Dako A0425), Ki67 (Dako A047), C1q (the first component of the complement cascade) (Dako A0136), and CD3 (T-cell marker; Dako A0452) polyclonal antibodies or mouse anti-human CD20 (B-cell marker; Dako M0755), CD8 (suppressor of cytotoxic T cells; Dako M7103), p63 (plasma cell marker; Dako M7077), and Ham56 (monocyte/macrophage marker; Dako M0632) monoclonal antibodies were used as primary antibodies.

The p63 protein is an intracellular type II transmembrane protein localized in the rough endoplasmic reticulum and expressed only by plasma cells among hematopoietic cells (54). However, p63 also binds melanocytic, epithelial, and endothelial cells (61). The following primary antibodies were used to study the expression of *Borrelia* proteins: mouse monoclonal antibodies H9724 for flagellin (3), H5332 for OspA (4), and H614 for OspB (4); rabbit hyperimmune serum to recombinant OspC (21); and rabbit antiserum 10060 to glutathione *S*-transferase– VlsE1c (fusion protein) for VlsE (33). For negative controls, duplicate sections on each glass slide were incubated with affinity-purified nonspecific IgG matched for concentration, species, and isotype. A section incubated with wash buffer (see below) instead of primary antibodies was included in all assays to control for nonprimary antibody-related background. The positive controls for inflammatory markers were spleen sections. The positive controls for *Borrelia* strains were frozen homogenates of cultured strain N40 in M-1 embedding matrix (Shandon). The secondary reagent was biotinylated goat anti-rabbit or goat anti-mouse polyclonal antibody (Biogenex). The tertiary reagent was horseradish peroxidase-labeled streptavidin (Biogenex). Incubation times were 30 min for the primary reagents and 20 min for the secondary and tertiary reagents. The chromogen was 3,3-diaminobenzidine tetrahydrochloride in 0.24% H_2O_2 and was used for 5 to 15 min. The counterstain was Mayer's hematoxylin in H_2O and was used for 1 min. No counterstain was used for image analysis immunostaining. Each incubation was separated by washes with OptiMax wash buffer (Biogenex). Sections from monkey spleens were used as positive controls. A catalase amplification system (Dako) was used for the detection of CD8. The intensity and extent of the immunohistochemical stains were compared by digital image analysis with Image-Pro Plus software, version 4.1. For this, a masked examiner (Y.B.) took three or four digital pictures at a magnification of ×40, ×100, or ×200 per microscopic section. The mean and SD sum area and the mean and SD sum optical density per microscopic field were determined and compared between groups for statistical significance. The area refers to the number of pixels positive for the signal of interest, while the optical density is used to correct for the relative intensity of each positive pixel. The sum is determined by adding the individual results for each of the fields measured per section.

Immunoblotting. One hundred milligrams of frozen skeletal muscle was sliced very thinly with a disposable scalpel and thawed in lysis buffer (see below) containing a cocktail of protease inhibitors. One milliliter of lysis buffer contained 950 μl of radioimmunoprecipitation assay buffer (see below), 10 μl of phenylmethylsulfonyl fluoride (10 mg/ml), 30 μl of aprotinin (Sigma A6279), and 10 μl of 100 mM sodium orthovanadate. Radioimmunoprecipitation assay buffer contained PBS, Igepal CA-630 nonionic detergent (Sigma), 0.5% sodium deoxycholate, and 0.1% sodium dodecyl sulfate. The tissues were further disrupted and homogenized with a Fast Prep system (Bio 101). After the addition of 30 μl of phenylmethylsulfonyl fluoride (10 mg/ml)/g, the tissue homogenates were incubated on ice for 30 min, followed by centrifugation at 4°C for 10 min at 10,000 × *g*. Protein concentrations in the supernatants were determined with the bicinchoninic acid protein assay (Pierce). Dot blots were prepared by spotting 0.1 to 1 μg in duplicate from each protein extract onto polyvinylidene difluoride membranes (Millipore), which were allowed to dry for 5 min at room temperature. After blocking for 1 h in 5% nonfat dried milk in Tris-buffered saline with 0.1% Tween 20 at room temperature, the membranes were incubated with primary antibodies for 1 h, washed three times, and incubated with secondary antibodies for an additional 1 h. The primary antibodies were rabbit anti-human IgG (Dako) or IgM polyclonal antibodies at a 1:5,000 dilution or anti-human Ki67 at a 1:100 dilution. The secondary antibodies were alkaline phosphatase-conjugated goat anti-rabbit IgG (Sigma) antibodies at a 1:5,000 dilution. Nonspecific affinity-purified IgG (Sigma) matched for concentration and isotype was used as a negative control. After incubation in fluorescence substrate enzyme-catalyzed fluorescence (Amersham Life Science RPN5785) for 5 min, the membranes were scanned with a Typhoon 8600 scanner (Amersham). The results were analyzed by densitometry with Image-Quant Software and expressed as the mean and SD. The results were compared for statistical significance by Student's *t* test.

RT-PCR. Total RNA was extracted from 100-mg tissue blocks or 20-μm-thick cryostat sections of frozen skeletal muscle with TRIzole reagent (Life Technologies). Reverse transcription (RT) was performed with 20-μl reaction volumes. The RT reaction mixture contained RT buffer (500 mM KCl, 100 mM Tris-HCl [pH 8.3]), 5.5 mM $MgCl_2$, 500 μM each dATP, dCTP, and dTTP, 200 μM reverse primer, 0.4 U of RNase inhibitor/μl, and 1.25 U of MultiScribe reverse transcriptase. One microliter of total RNA was used as a template for RT. Cycling parameters for RT were 40 min at 48°C and 5 min at 95°C. PCR primers and the TaqMan probe and primers were designed with Primer Express software (Perkin-Elmer Applied Biosystems, Foster City, Calif.).

For *Borrelia* quantitation, real-time TaqMan RT-PCR was used. Multiple 16S rRNA Lyme disease and relapsing fever *Borrelia* sequences available from GenBank were aligned, and primers were chosen to target a 136-bp-long segment common to many *Borrelia* spp. The forward primer corresponds to the *B. burgdorferi* B31 16S rRNA sequence from bp 739 to 760 (5′-GGTCAAGACTGAC GCTGAGTCA-3′; GenBank accession number U03396). The reverse primer corresponds to bp 874 to 853 (5′-GGCGGCACACTTAACACGTTAG-3′). The fluorogenic probe corresponds to bp 801 to 829 (6FAM-5′-TCTACGCTGTAA ACGATGCACACTTTGGTG-3′-TAMRA). For NHP glyceraldehyde-3-phosphate dehydrogenase (GAPDH), the forward primer was 5′-CCAGTGGACTC CACGACGTA-3′, the reverse primer was 5′-GCGAGATCCCTCCAAAATC A-3′, and the fluorogenic probe was VIC (5′-AGCGCCAGCATCGCCCCAC-3′).

The TaqMan PCR mixture contained TaqMan Universal PCR Master Mix (Perkin-Elmer Applied Biosystems PN.4304437), 100 μM 16S probe, 200 μM 16S forward primer, 200 μM 16S reverse primer, and 10 μl of cDNA as a template. Samples were run in duplicate. Amplification and detection were performed with an ABI 7700 system (Perkin-Elmer Applied Biosystems) with the following cycling conditions: uracil *N*-glycosylase incubation at 50°C for 2 min, AmpliTaq gold activation at 95°C for 5 min, and 50 cycles of denaturation at 95°C for 15 s and annealing-extending at 60°C for 1 min. For quantification of the spirochetal load, strain N40 spirochetes were cultured in vitro and counted in a Petroff-Hausser chamber by phase-contrast microscopy. RNA was extracted from known numbers of spirochetes, added to RNA extracted from skeletal muscle from noninfected NHPs (to control for PCR inhibition by host nucleic acid), and used in $\log_{10}$ dilutions to obtain a linear-range reference curve with a coefficient of ≥0.98. PCRs with H_2O instead of cDNA were included as negative controls. A cycle threshold (Ct) of 40 was required in all negative controls for the assay to be valid.

For C1q (GenBank accession number X03048) PCR, we used a forward primer corresponding to the sequence from bp 349 to 369 (5′-CTGGCTAGAC CATGGTGAGTT-3′) and a reverse primer corresponding to bp 862 to 881 (5′-AAGATGCTGTTGGCACCCTC-3′), with a predicted fragment size of 532 bp. The GAPDH (GenBank accession number BC029618) forward primer corresponds to the human GAPDH sequence from bp 65 to 89 (5′-TGAAGGTC GGAGTCAACGGATTTGG-3′). The GAPDH reverse primer corresponds to the human GAPDH sequence from bp 440 to 462 (5′-GTTCACACCCATGAC GAACATGG-3′).

RT-PCR amplification was carried out with a 25-μl reaction mixture containing PCR buffer minus Mg (Applied Biosystems PN.808-0234), 2.5 U of *Taq* DNA polymerase (5 U/μl; Invitrogen catalog no. 10342-053), 200 μM deoxynucleoside triphosphates (dNTPs), 2 mM $MgCl_2$, and 0.5 μM each specific primer. The mixture was prepared before the addition of 1 μl of cDNA. PCR amplification was carried out with a GeneAmp PCR system 9700 (Perkin-Elmer Applied Biosystems). The amplification program consisted of an initial denaturation step at 94°C for 5 min. The remaining cycles were 1 min at 94°C, 30 s at 58°C, and 30 s at 72°C. The number of cycles performed was 40. Final extension was done for 5 min at 72°C. After amplification, PCR products were stained with ethidium bromide and measured with a Typhoon 8600 scanner. Results were expressed as the densitometry ratio of the C1q bands to the GAPDH bands.

Statistical analysis. Differences in mean sum area or density between groups were compared for statistical significance with Student's *t* test and Excel software. A two-tailed analysis was used for all measures. A *P* value of equal or less than 0.05 was considered significant.

RESULTS

Animal infections. A total of 16 NHPs inoculated with *B. burgdorferi* were included in these studies (Table 1). Two

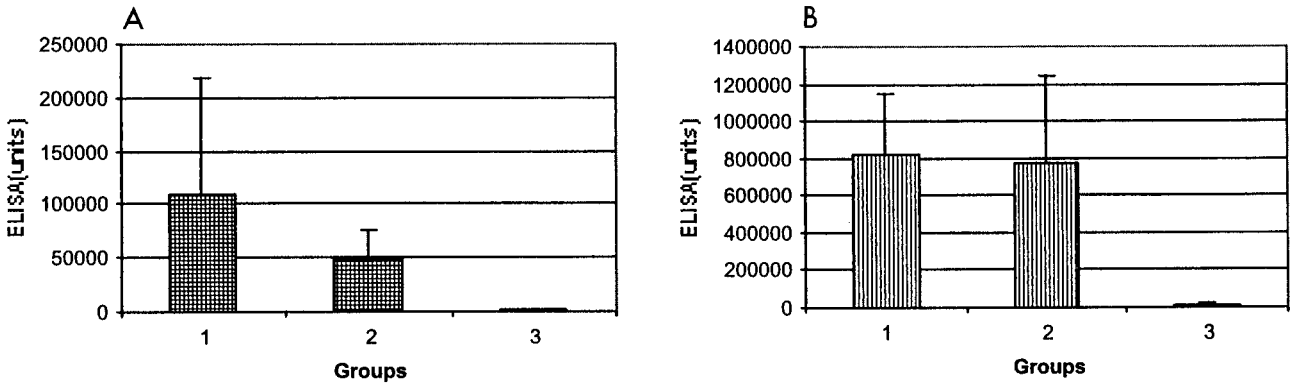

FIG. 2. *B. burgdorferi*-specific antibodies of the IgM (A) or IgG (B) isotype in necropsy sera from TISP NHPs 90 days after inoculation with *B. burgdorferi* sensu stricto strain N40 by needle (group 1) or by tick bite (group 2) or with *B. garinii* strain Pbi by needle (group 3). An ELISA was carried out with homologous sonicates and sera diluted 1:500. Data are reported as means and SDs.

strains were used for inoculation. *B. burgdorferi* sensu stricto strain N40 was used in previous studies with the NHP model of Lyme disease (40–42). For the first time, some NHPs were inoculated with strain N40 by tick bite rather than by needle. The second strain was *B. garinii* strain Pbi. Strain Pbi is a human cerebrospinal fluid isolate from Germany (29, 63, 67). Prior to inoculation into NHPs, strain Pbi was tested in outbred Swiss Webster mice and found to be infectious by culturing in BSK-H medium of bladder and/or heart tissues obtained at necropsy 1 month after inoculation. All but two NHPs were immunosuppressed with dexamethasone to increase the probability that they would become infected. The two NHPs that remained IC were necropsied 120 days after inoculation. Four NHPs necropsied 50 days after inoculation, while they were still receiving dexamethasone, were designated IS (Fig. 1). Ten NHPs necropsied 90 days after inoculation, 40 days after dexamethasone had been discontinued, were designated TISP.

Specific antibody response. The two IC NHPs inoculated with strain N40 developed a strong but transient specific antibody response (data not shown). A serum ELISA with homologous whole-cell sonicates showed that all TISP NHPs inoculated with strain N40 by needle (group 1) or by tick bite (group 2) had specific antibodies at the time of necropsy (Fig. 2). The levels of specific IgM or IgG antibodies were not significantly different whether strain N40 was inoculated by needle (group 1) or by tick bite (group 2) (Fig. 2). In contrast, the specific antibody response in sera from the two strain Pbi-inoculated TISP NHPs (group 3) was much weaker (Fig. 2). Examination of the sera from the two strain Pbi-inoculated TISP NHPs by an ELISA at a dilution lower than the standard dilution (1:500 instead of 1:5,000) showed the presence of specific antibodies in both animals (Fig. 3). However, serum Western blotting was negative for both animals even when homologous recombinant immunoblotting was used (Bettina Wilske, personal communication).

Spirochetal load. Three methods were used to investigate infection in skeletal muscle. First, skeletal muscle needle biopsy specimens obtained at necropsy were cultured in BSK-H medium. All cultures from the IC and TISP NHPs were negative. Unfortunately, the cultures from the IS NHPs were contaminated. Second, we examined skeletal muscle infection by microscopy of immunostained sections. For this, frozen muscle sections stained with hyperimmune sera from a strain N40-infected rabbit were examined for the presence of spirochetes by light microscopy. Spirochetes were observed only in muscles from the two strain N40-inoculated IS NHPs (Fig. 4). All muscle sections examined from these two NHPs (no. 794 and 372) had large numbers of spirochetes, as many as 5 to 10 per ×400 microscopic field. They were localized predominantly in connective tissue (endomysium, perimysium, and epimysium). In no case did they appear to be localized intracellulary in muscle fibers. Immunohistochemical analysis with various monoclonal and polyclonal antibodies revealed that these spirochetes did not express OspA, OspB, or OspC. The expression of flagellin was a consistent feature, but the expression of VlsE appeared weak and was not seen consistently (data not shown). This pattern of VlsE expression also was seen in the cultured spirochetes used as a positive control. This finding likely can be explained by significant differences between VlsE from *B. burgdorferi* strain B31 (used to immunize the rabbit to produce the anti-VlsE polyclonal antibody used for these experiments) and VlsE from strain N40. Our failure to amplify N40 VlsE with primers from B31 VlsE is evidence of this notion (data not shown).

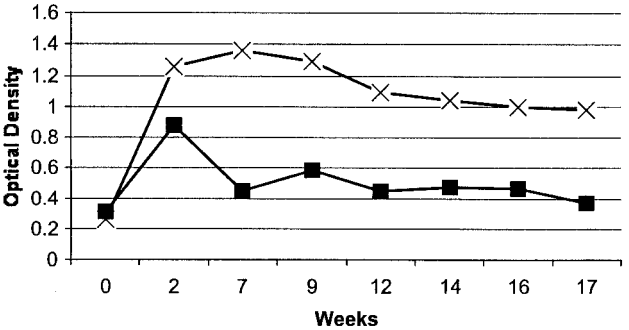

FIG. 3. Total specific antibody production in TISP NHPs 105 (×) and 321 (■) after intradermal inoculation with *B. garinii* strain Pbi. An ELISA was carried out with homologous sonicates and sera diluted 1:200.

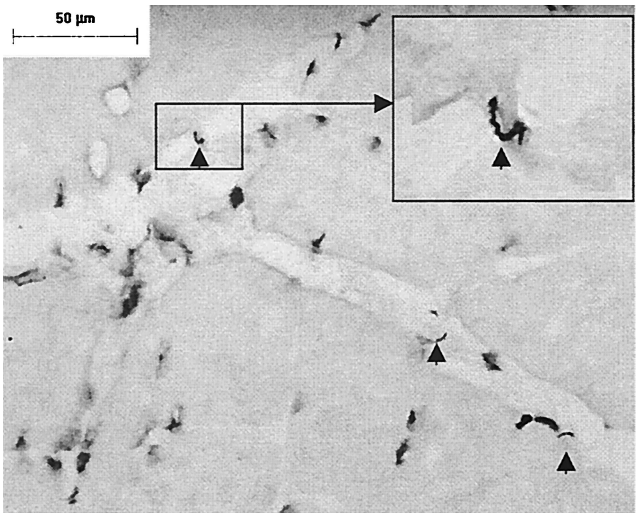

FIG. 4. *B. burgdorferi* sensu stricto strain N40 in skeletal muscle from an IS NHP 50 days after intradermal inoculation. Arrowheads indicate spirochetes in the endomysium. Immunohistochemical analysis was carried out with hyperimmune rabbit serum. Magnifications, ×360 in the main panel and ×900 in the inset. Bar, 50 μm.

The culture and immunohistochemical data indicated that if muscles from IC or TISP NHPs were infected, the spirochetal load would be very low. To investigate this possibility, we examined them with a sensitive and specific TaqMan RT-PCR that targets the 16S rRNA of *Borrelia* spp. (Table 2). This assay consistently detects <10 spirochetes/500 ng of host DNA (40). For this assay, we extracted whole RNA from 100-mg blocks of frozen skeletal muscle from all NHPs. A standard curve with RNA extracted from $\log_{10}$ dilutions of known numbers of strain N40 spirochetes was used for quantification. To control for the possibility of inhibition by host nucleic acid, PCR amplification was done in the absence or in the presence of 1 μg of host DNA added to the standard-curve sample. To examine for the possibility of variations in spirochetal load within the same muscle, two different areas were tested. The results showed that the number of spirochetes per microgram of skeletal muscle RNA in all TISP NHPs was very low. In all but one case, strain N40-inoculated TISP NHPs had <1 spirochete/μg of RNA. No spirochetes were detected in any of the skeletal muscles examined from IC NHPs (four of four samples had Ct values of 40) or from two uninfected NHPs used as negative controls (four of four samples had Ct values of 40). In contrast, TaqMan results for all samples examined from the strain N40-inoculated IS NHPs showed a very large spirochetal load, with values of 38,795 to 500,290 spirochetes per 500 ng of host RNA. The mean (SD) numbers of spirochetes in biceps and quadriceps muscles from these two animals were 2.2×10^5 (1.6×10^5) and 7.4×10^5 (3.5×10^5), respectively.

Inflammation in skeletal muscle. Biceps and quadriceps muscles from all NHPs were examined for the presence of inflammation (myositis) by light microscopy of HE-stained frozen and paraffin sections. The results (Table 1) showed that all strain N40-inoculated TISP NHPs had myositis. In contrast, none of the strain N40-inoculated IC NHPs and none of the strain Pbi-inoculated NHPs had evidence of myositis in any of the more than 10 sections examined per muscle per animal. Only one of the two strain N40-inoculated IS NHPs had myositis, which was mild. No myositis was seen in any of the negative control skeletal muscles. The inflammatory infiltrates in the strain N40-TISP NHPs were predominantly perivascular and interstitial, and occasionally skeletal muscle fiber degeneration was seen (Fig. 5A). The severity of inflammation in TISP NHPs needle inoculated versus tick inoculated with

TABLE 2. Spirochetal load determined by quantitative TaqMan RT-PCR for *Borrelia* 16S rRNA in biceps muscle from NHPs inoculated with borreliae[a]

NHP no.	Strain	Inoculation	Results obtained in the absence or presence of host nucleic acid added to the standard-curve sample used for *Borrelia* measurements[b]					
			Absence		Presence			
					Sample 1		Sample 2	
			Input μg of RNA	Load	Input μg of RNA	Load	Input μg of RNA	Load
099	N40	Needle	1.2	0.0002	1	0	1	0.1500
177			3.8	0.0001	1	0	1	0.0300
199			2.7	0.0101	1	0.0037	1	0.0300
383			3.4	0.0113	1	0	1	0.0100
154	N40	Tick bite	2.1	0.0016	1	0.0011	1	0.4000
192			2.6	0.0043	1	0.0019	1	1.6000
211			2.7	0.0048	1	0	1	0.0200
242			2	0.0007	1	0	1	0
105	Pbi	Needle	Not done		1	0.0020	1	0.0300
321			Not done		1	0.0011	1	0.0200
012			Not done				0.5	0
981			Not done				0.5	0

[a] NHPs were inoculated with *B. burgdorferi* sensu stricto strain N40 or *B. garinii* strain Pbi. Load is reported as number of spirochetes per microgram of skeletal muscle RNA.

[b] One microgram of host nucleic acid was added to the standard-curve sample to control for the possibility of PCR inhibition by host nucleic acid. In the presence of host nucleic acid, a different areas of the biceps muscle (samples 1 and 2) were examined to search for variations in spirochetal loads between different areas of the same muscle.

strain N40 was compared by a masked examiner (D.C.) using light microscopy of HE-stained sections (Table 3). A score of 0 to 4+ for the number of inflammatory foci was used (see Materials and Methods for details). The results showed that myositis was significantly more severe in needle-inoculated than in tick-inoculated TISP NHPs. In needle-inoculated TISP NHPs, five of eight sections had a score of ≥2; in contrast, in tick-inoculated TISP NHPs, five of eight sections had a score of <1 ($P < 0.05$). To confirm these observations, the severity of inflammation was also compared by digital image analysis of Ki67-immunostained sections (Fig. 5D) by a different masked examiner (Y.B.) (Table 3). The results showed that the mean sum area in square micrometers positive for Ki67 immunostaining was significantly larger in needle-inoculated than in tick-inoculated TISP NHPs (5.9×10^3 versus 2×10^3) ($P < 0.0001$). The coefficient of correlation between the severity of myositis (measured by Ki67 immunostaining) and the spirochetal load (measured by TaqMan RT-PCR) was only 0.36.

Analysis of cellular inflammatory infiltrates. Microscopic examination of HE-stained muscle sections revealed significant skeletal muscle inflammation in strain N40-inoculated TISP NHPs (Table 3). In addition to mononuclear cells, there were also numerous cells with the characteristic morphological features of plasma cells. To further characterize the inflammatory infiltrates in strain N40-inoculated TISP NHPs, we used immunostaining for T cells (CD3) (Fig. 5B), B cells (CD20), plasma cells (p63) (Fig. 5C), and macrophages (Ham56). Light microscopic examination indicated that the predominant inflammatory cells were T cells and plasma cells. Immunostaining with anti-CD8 monoclonal antibody showed that the majority of T cells were $CD8^+$ (data not shown). Digital image analysis was used to compare the extent of T-cell and plasma cell infiltration in the three groups of TISP NHPs, groups 1 to 3. The results showed that there was significantly more CD3 (Fig. 6A) and p63 (Fig. 6B) immunostaining in skeletal muscle from groups 1 and 2 than in that from group 3. When groups 1 and 2 were compared, significantly more CD3 immunostaining was found in group 1 ($P < 0.01$). In contrast, there was no difference in p63 immunostaining between groups 1 and 2. The p63-positive immunostaining observed for group 3 TISP NHPs (Fig. 6B) originated mainly from connective tissue of the endomysium and perimysium, whereas no cells with morphological features of plasma cells were identified on HE-stained sections. This signal appeared to originate from endothelial cells, which can be p63 positive (61).

Next, we selected one of the group 1 NHPs (no. 199) to compare the extent of T-cell (CD3) and plasma cell (p63) infiltration in muscle with that of B-cell (CD20) and macrophage (Ham56) infiltration and to measure cellular proliferation (Ki67) (Fig. 6C). CD3 and p63 were significantly more prevalent than CD20 or Ham56. The mean and SD sum areas in square micrometers per ×40 microscopic field were 13,942 ± 2,945 for p63, 10,375 ± 4,086 for CD3, 418 ± 340 for CD20, and 268 ± 118 for Ham56. The corresponding value for the cellular proliferation marker Ki67 was also increased, at 3,656 ± 1,860, but was lower than that of CD3 or p63. These results indicated that significant numbers of CD3- or p63-positive cells were not proliferating.

Digital image analysis of molecular inflammatory infiltrates. Plasma cells were abundant in skeletal muscle from TISP NHPs infected with strain N40 by tick bite or needle. Since the production of immunoglobulin is the primary function of plasma cells, we next searched for the presence of antibody and complement in inflamed muscles from strain N40-inoculated TISP NHPs (groups 1 and 2) and compared the findings with those for muscles with no evidence of inflammation in the strain Pbi-inoculated TISP NHPs (group 3). Light microscopic examination revealed extensive deposition of IgM (Fig. 5E) and IgG (Fig. 5F) in muscle membranes and blood vessels and in connective tissue (endomysium and perimysium) from inflamed but not from noninflamed muscles. Digital image analysis of frozen sections immunostained with antibodies specific for IgM, IgG, or C1q was used to compare the extent of antibody and complement deposition in these three TISP groups (Fig. 7). The mean sum areas positive for IgM deposition in square micrometers per ×40 microscopic field were 8.5×10^5, 1.8×10^5, and 4.6×10^3 for groups 1, 2, and 3, respectively. IgM deposition was significantly higher for groups 1 and 2 than for group 3 (the P value was 0.017 for group 1 versus group 3, and the P value was 0.04 for group 2 versus group 3). IgM deposition was also significantly higher for group 1 than for group 2 ($P = 0.007$). There were also significant differences in IgG deposition. The mean sum areas positive for IgG deposition in square micrometers per ×40 microscopic field were 1.12×10^6, 1.28×10^6, and 8.3×10^5 for groups 1, 2, and 3, respectively (the P value was 0.001 for groups 1 and 2 versus group 3). In contrast to the findings for IgM, there was no significant difference in IgG deposition between groups 1 and 2. The results showed there was also deposition of the C1q complement protein, although it was much lower than that of IgM or IgG (Fig. 7). C1q deposition was significantly higher in groups 1 and 2 than in group 3 ($P < 0.001$) and in group 1 than in group 2 ($P = 0.04$). C1q was localized predominantly in the endomysium and perimysium (data not shown), similar to IgM and IgG (Fig. 5E and F). These results revealed significant deposition of antibody and complement in inflamed skeletal muscle from strain N40-inoculated NHPs.

Analysis of antibody deposition in skeletal muscle by immunoblotting. Digital image analysis of immunostained sections showed significantly increased deposition of antibody and complement in inflamed muscle from strain N40-inoculated TISP NHPs. However, digital image analysis can measure only small areas of tissue at a time. To compare antibody deposition in larger tissue samples, we used quantitative densitometry of fluorescent dot blots. For this, 1 mg of whole protein extracts from 100-mg tissue blocks per muscle per animal was dot blotted in triplicate on polyvinylidene difluoride membranes and probed with IgG- or IgM-specific antibodies, and the relative fluorescence of each dot was measured by densitometry with a Typhoon 8600 scanner. The results are summarized in Table 4. The amounts of IgG and IgM were higher in strain N40-inoculated TISP NHPs than in strain Pbi-inoculated TISP NHPs. The amount of IgG was significantly higher in group 1 than in group 2 ($P < 0.0001$) or group 3 ($P = 0.007$). The amount of IgM was significantly higher in groups 1 and 2 than in group 3 (the respective P values were 0.003 and 0.01). Group 1 had more IgM than group 2, but the difference did not reach statistical significance ($P = 0.08$). A similar dot blot analysis for C1q could not be done because of insufficient sensitivity of the

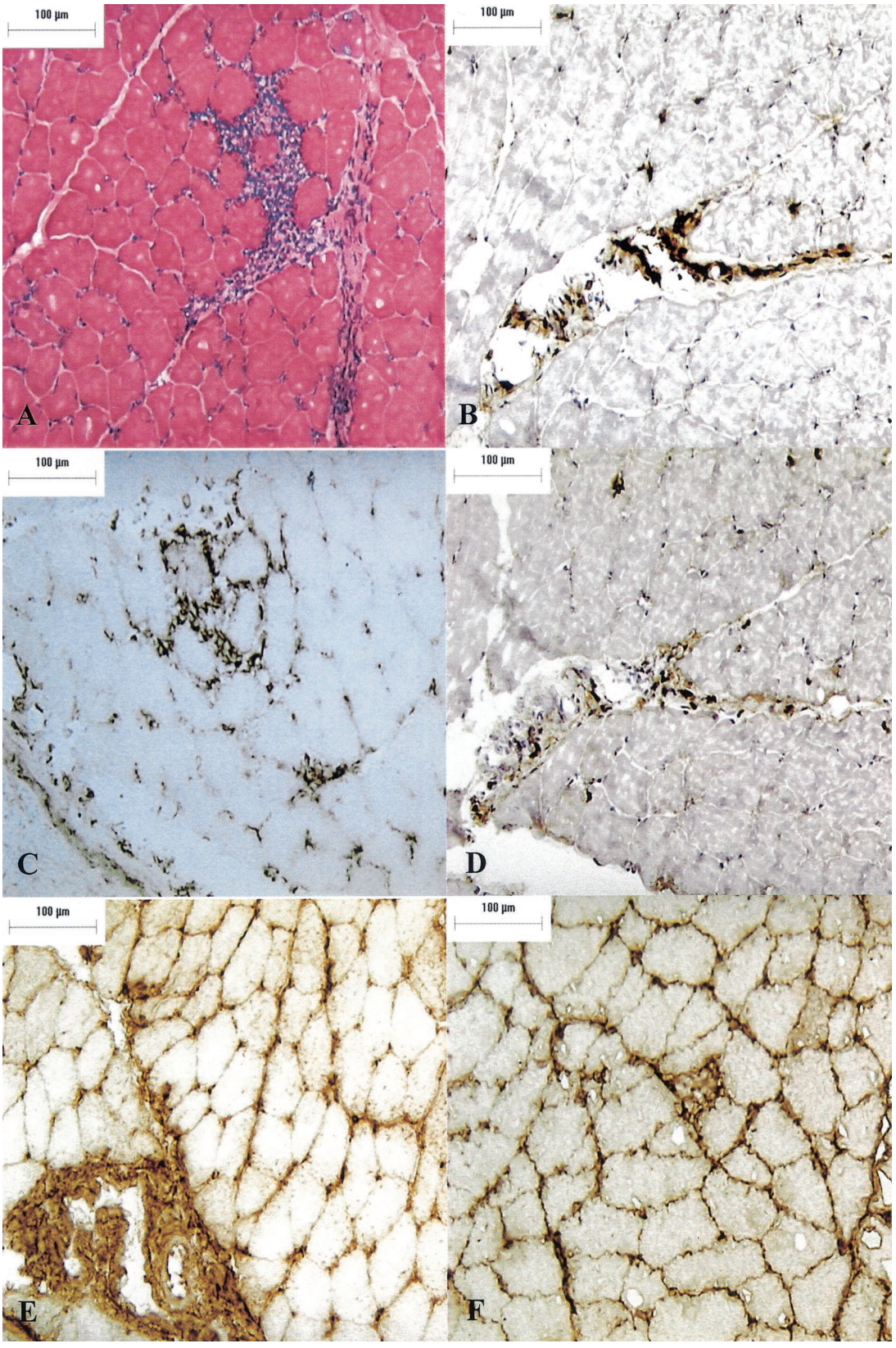

FIG. 5. Myositis in a TISP NHP 90 days after needle inoculation with *B. burgdorferi* sensu stricto strain N40. (A) HE stain (magnification, ×400). (B) T-cell immunostain (CD3) (magnification, ×200). (C) Plasma cell immunostain (p63) (magnification, ×200). (D) Ki67 immunostain (magnification, ×200). (E) IgM immunostain (magnification, ×200). (F) IgG immunostain (magnification, ×200). Bar, 100 µm.

TABLE 3. Severity of inflammation in skeletal muscle from TISP NHPs inoculated with *B. burgdorferi* strain N40 by needle or by tick bite

NHP no.	Group	Muscle examined	Inflammation[a]	Proliferation[b]
099	Needle	Biceps	1+	6.7 ± 1.0
		Quadriceps	2+	
177		Biceps	1+	4.2 ± 0.3
		Quadriceps	2–3+	
199		Biceps	2+	8.7 ± 1.3
		Quadriceps	2+	
383		Biceps	1+	4.1 ± 1.6
		Quadriceps	2+	
154	Tick bite	Biceps	0–1+	2.2 ± 3.0
		Quadriceps	0–1+	
192		Biceps	1+	2.0 ± 1.4
		Quadriceps	0	
211		Biceps	1+	2.0 ± 2.1
		Quadriceps	0	
242		Biceps	0	1.8 ± 0.6
		Quadriceps	1+	

[a] Severity of inflammation was graded from 0 to 4+ on HE-stained slides, as determined by masked examiner (see Materials and Methods for details).
[b] Mean and SD sum area in 10^3 square micrometers per ×40 microscopic field, as determined by masked digital image analysis of Ki67-immunostained sections (different sections from the same block as that used for HE staining).

assay (data not shown). This analysis with whole skeletal muscle protein extracts confirmed significantly increased antibody deposition in inflamed skeletal muscle from strain N40-inoculated TISP NHPs.

Measurement of total antibody in serum. The finding of increased deposition of antibody in inflamed muscle from strain N40-inoculated TISP NHPs raised a question regarding the source of this antibody. One possibility was that it was produced locally by the large number of plasma cells found in inflamed skeletal muscle (Fig. 5C and 6B). An alternative (or complementary) source was circulating antibody produced by plasma cells present in the lymph nodes, spleen, or other lymphoid organs or sites of chronic inflammation (55). To investigate these possibilities, we measured the amounts of total circulating antibodies in necropsy sera for the three groups of TISP NHPs. The results (Fig. 8) showed that the amounts of total IgM antibodies in necropsy sera were significantly higher in groups 1 and 2 than in group 3 (the respective *P* values were 0.02 and 0.05). The amounts of total IgG antibodies in necropsy sera from groups 1 and 2 were also higher than those for group 3, but the differences did not reach statistical significance (the respective *P* values were 0.07 and 0.34). These results showed increased total antibody levels in N40-inoculated TISP NHPs and suggested that one potential source of IgM antibodies deposited at sites of chronic inflammation, including skeletal muscles, is circulating antibodies.

Measurement of C1q expression in muscle by RT-PCR. Digital image analysis of immunostained sections showed increased deposition of C1q in muscle, but this finding could not be confirmed by dot blot analysis because of insufficient sensitivity. Therefore, we used RT-PCR to compare the amounts of C1q gene expression in skeletal muscle from the three groups of TISP NHPs. The results, expressed as the mean and SD ratio of C1q densitometry to GAPDH densitometry (×100) in the respective RT-PCR products, were 74.6 ± 1.2, 72.7 ± 8.8, and 48.3 ± 3.6, respectively, for groups 1, 2, and 3. The differences between groups 1 and 3 and between groups 2 and 3 were statistically significant (the respective *P* values were 0.05 and 0.02). These results confirmed that C1q deposition was increased in inflamed skeletal muscle from N40-inoculated TISP NHPs. Just as important, since mRNA was measured, they revealed that C1q was actually being synthesized in muscle and was not merely being deposited from the circulation.

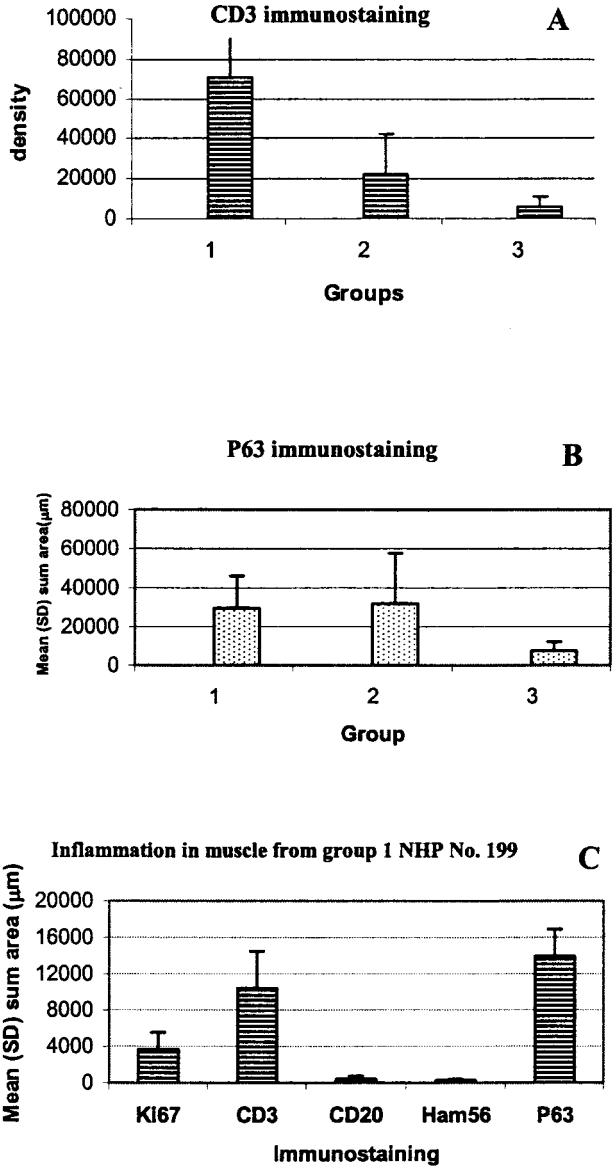

FIG. 6. CD3 (A) or p63 (B) immunostaining in skeletal muscle from TISP NHPs inoculated with strain N40 by needle (group 1) or by tick bite (group 2) or with strain Pbi by needle (group 3). Results are given as mean and SD sum density in arbitrary units (CD3) or sum area in square micrometers per ×40 microscopic field (p63). (C) Immunostaining for various inflammatory markers in skeletal muscle from a strain N40 needle-inoculated TISP NHP (no. 199), shown in mean and SD square micrometers per ×40 microscopic field. Ki67, proliferation marker; CD3, T-cell marker; CD20, B-cell marker; Ham56, macrophage marker; p63, plasma cell marker.

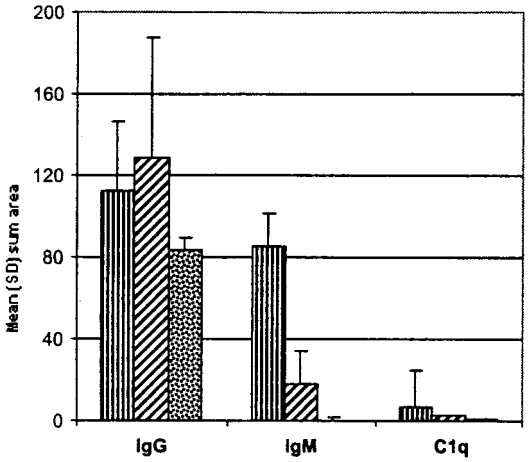

FIG. 7. Comparison of antibody (IgG and IgM) and complement (C1q) deposition in skeletal muscle from TISP NHPs inoculated with strain N40 by needle (group 1; ▥) or by tick bite (group 2; ▨) or with strain Pbi by needle (group 3; ▩). Results are given as mean and SD sum area in 10^4 square micrometers per ×40 microscopic field.

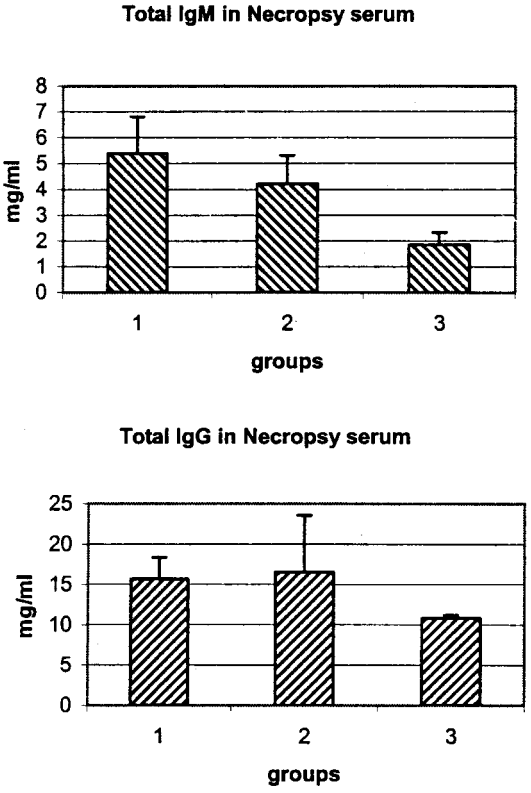

FIG. 8. Total antibodies of the IgM (A) or IgG (B) isotype in necropsy sera from TISP NHPs inoculated with strain N40 by needle (group 1) or by tick bite (group 2) or with strain Pbi by needle (group 3). Data are reported as mean and SD.

DISCUSSION

This article presents a comprehensive investigation of skeletal muscle involvement in experimental Lyme borreliosis in NHPs. The focus was on skeletal muscle because prior studies showed that skeletal muscle has the highest spirochetal load of any tissue examined in NHPs inoculated with *B. burgdorferi* (11). Our studies over the years with strain N40 have shown that IC NHPs are relatively resistant to Lyme borreliosis (40, 42, 44, 45). This was in fact the case with the two IC NHPs examined in this study, which developed a strong and early specific antibody response and showed no evidence of infection or inflammation in skeletal muscles at necropsy. Therefore, we used different degrees of immunosuppression to study both infection (in IS NHPs) and the host inflammatory response (in TISP NHPs).

The main findings of the study were as follows. (i) Depending on the immune status, strain N40 spirochetes inoculated into NHPs can fail to infect muscle and cause no tissue injury (IC NHPs), can result in a high level of persistent infection with no inflammation or little inflammation (IS NHPs), or can cause significant inflammation with minimal if any residual infection (TISP NHPs). (ii) The inflammatory response in skeletal muscle from TISP NHPs is significantly lower when spirochetes are inoculated by tick bite rather than by needle, mostly as a result of decreased T-cell levels. (iii) The predominant cells of the inflammatory response in inflamed muscles from TISP NHPs are T cells (mostly $CD8^+$) and plasma cells. (iv) Inflamed muscles from TISP NHPs have significant deposition of immunoglobulins and C1q. (v) Strain Pbi is significantly less infectious for NHPs than strain N40.

TABLE 4. IgG and IgM levels in perfused skeletal muscle from NHPs, as determined by: quantitative dot blot analysis[a]

Group	Amt of:	
	IgG	IgM
1	4.3 ± 0.1[b,c]	0.7 ± 0.2[b]
2	3.1 ± 0.1	0.5 ± 0.02[d]
3	3.6 ± 0.3	0.3 ± 0.06

[a] NHPs were inoculated with strain N40 by needle (group 1) or by tick bite (group 2) or with strain Pbi by needle (group 3). Data are reported in arbitrary density units as mean densities and SDs (10^7).
[b] The *P* value was <0.01 for a comparison between group 1 or 2 and group 3.
[c] The *P* value was <0.01 for a comparison between groups 1 and 2.
[d] The *P* value was <0.05 for a comparison between group 1 or 2 and group 3.

Myositis developed in TISP NHPs but not IS NHPs, probably because the continuous use of steroids inhibited the muscle inflammatory response to the infection. The reason why myositis developed in strain N40-inoculated TISP NHPs but not in strain Pbi-inoculated TISP NHPs is less clear. The most likely explanation is that strain Pbi was less infectious for NHPs than strain N40. This notion is supported by the finding that only one out of four Pbi-inoculated TISP NHPs developed a significant specific antibody response (Table 1). Furthermore, a sensitive TaqMan assay consistently found between 0 and <1 spirochete/μg of RNA in all muscles tested from Pbi-inoculated NHPs (Table 2), confirming a very low spirochetal load despite absent or lower specific antibody titers. Another possibility is that Pbi-inoculated NHPs were not capable of mounting an effective humoral and cellular inflammatory response to the infection. Contrary to most laboratory mice, NHPs are outbred and may have heterogeneous immune responses to *Borrelia* infection. We believe that this possibility is unlikely, because in such a case, a higher spirochetal load

would be expected. Furthermore, all rhesus macaques inoculated with strain Pbi were from the same colony, of the same sex, and of a similar age as those inoculated with strain N40. Additionally, examination of other tissues from strain Pbi-inoculated NHPs showed that at least one of them had significant inflammation characteristic of Lyme borreliosis in other organs (meningoradiculitis) (NHP no. 321; unpublished results). Finally, another possibility is that the development of myositis in strain N40-inoculated TISP NHPs was the result of a higher spirochetal load in infected muscles early during the immunosuppressive phase, leading to a more severe inflammatory response after the steroids were tapered off. Previous studies indicated a positive correlation between inflammation and the spirochetal load in tissues from antibody-deficient mice persistently infected with the relapsing fever agent *Borrelia turicatae* (12, 13).

There were several significant differences in the inflammatory responses in skeletal muscles from TISP NHPs inoculated with strain N40 by needle versus by tick bite. Overall, the level of inflammation was lower in tick bite-inoculated NHPs. Although tick bite-inoculated TISP NHPs had lower levels of T-cell infiltration and IgM and C1q deposition, the level of plasma cell infiltration was similar to that in needle-inoculated NHPs. One possibility is that these differences can be explained by different numbers of spirochetes being inoculated by needle versus by tick bite. However, our estimates of the numbers of spirochetes inoculated by tick bite (see Materials and Methods) were similar to those delivered by needle. Another possibility is that inoculation by tick bite was immunosuppressive for the NHPs in addition to the effect of the steroids on the immune system. In C3H/He J mice infected with *B. burgdorferi*, tick infestation results in the upregulation of interleukin 4 (IL-4) and IL-10 and in the downregulation of IL-2 and gamma interferon (65). In hamsters, the antibody response to tick-transmitted *B. burgdorferi* is different from that to needle-inoculated cultured spirochetes (50). A similar phenomenon has been noted for NHPs inoculated with *B. burgdorferi* (46).

The finding of multifocal collections of lymphocytes and plasma cells in perivascular locations is consistent with the pathology of Lyme borreliosis in humans (19, 58) and experimental animals, including rodents (66) and NHPs (11). Plasma cells during infection are prominent in lymph nodes, the spleen, and sites of chronic inflammation (55). They are cellular factories devoted entirely to the manufacture and export of a single product, soluble immunoglobulins. The life span of plasma cells varies from a few days to many months (14). Plasma cells are consistently found in tissues chronically infected with many different pathogens, including parasites and viruses (1, 20). The continuing presence of plasma cells may be an indication that low numbers of spirochetes are still present in TISP NHPs. In support of this notion is the finding that very low but detectable amounts of spirochetal RNA were found in TISP muscles by TaqMan RT-PCR (Table 2). The continuous production of specific antibodies by long-lived plasma cells may be a requirement for keeping the spirochetal load at such low levels.

One of the consequences of inflammation in strain N40-inoculated TISP NHPs was increased deposition of antibodies and complement. There are at least two potential sources of these antibodies—plasma cells which, as mentioned earlier, are abundant in inflammatory lesions (Fig. 5C), and circulating antibodies (Fig. 8). Both IgM and IgG are capable of activating complement and may be responsible for some of the tissue injury observed in neuroborreliosis. The specificity of the excess antibodies found in tissues and in the blood is not known but probably includes both specific and nonspecific antibodies. *B. burgdorferi* is a well-known polyclonal B-cell activator (53).

The level of C1q was also found to be increased in inflamed muscles. C1q, the collagen-like and Fc-binding component of the complement system, is synthesized mainly in macrophages and epithelial cells, although endogenous production by cardiac (64) and skeletal (34) muscle fibers has been reported. Its synthesis by skeletal muscle fibers is upregulated by stimulation with gamma interferon (34) or after ischemia (64). C1q is a large and complex protein that, besides functioning as the first component of the classical pathway of complement activation, also can induce the production of cytokines (IL-6) and chemokines (IL-8) important for the acute-phase response and the recruitment of inflammatory cells (62). C1q-containing immune complexes can bind via a specific receptor for C1q (C1qR) to various cells, including endothelial cells, fibroblasts, and epithelial cells. C1q binding to its receptor (C1qR) enhances the secretion of immunoglobulins by plasma cells. The C1qR that enhances phagocytosis, C1qRP, is expressed in cells of the myeloid lineage, endothelial cells, and platelets (37). Nearly all humans with Lyme borreliosis have abnormal serum C1q-binding activity from the onset of erythema migrans, and this activity is persistent in patients with subsequent nerve or heart involvement (24, 25). Peripheral neuropathy observed in rhesus macaques infected with *B. burgdorferi* correlated in the most severely affected monkey with the presence of higher levels of C1q-binding immune complexes (49). Our data support the view that C1q production and deposition may be important components of the inflammatory response that may lead to tissue injury during neuroborreliosis.

Studies by various investigators with IS NHPs (11) and rodents by silver staining (7) and electron microscopy (38) have shown that *B. burgdorferi* has a tropism for the extracellular collagenous matrix of many tissues. This property also has been observed for human Lyme disease, in the skin (8), skeletal muscle (47), and synovium (30). In the present study, we observed spirochetes by immunohistochemical analysis only in muscles from IS NHPs which were found to have a very high spirochetal load by TaqMan RT-PCR. This finding suggests that C3H mice, which are commonly used for studies of experimental murine Lyme borreliosis and in whose tissues spirochetes are easily found by light microscopy, resemble more closely our IS NHPs than IC NHPs or TISP NHPs. Humans with Lyme borreliosis, in whom spirochetes are very difficult to find in tissues (26), except early during the infection or after dissemination only when very sensitive assays such as PCR are used (22), resemble more closely our IC NHPs or TISP NHPs.

Relatively little is known about skeletal muscle involvement in humans with Lyme borreliosis. It has been reported to occur from 7 weeks to 5 months after the initial infection (17, 18). In early Lyme disease, muscle pain, together with debilitating malaise and fatigue, is one of the most frequent clinical features. The pain is intermittent and generally migratory, involving not only muscles but also joints and tendons. In one study

in the United States 42% of 312 patients with Lyme borreliosis complained of myalgia, and 4% had muscle tenderness on examination (59). Myalgia may persist after inadequate treatment with antibiotics (31). Some patients complain of swelling of proximal muscles, such as those in the thighs. It is said to be characteristically localized to the vicinity of skin lesions, arthritis, or neuropathy (28, 47), although myositis affecting all limbs has been reported (47). The majority of patients have normal creating phosphokinase values (28). It has been reported to mimic dermatomyositis (27). Muscle biopsy specimens obtained in a few cases show collections of lymphocytes and plasma cells tightly packed around branches of the intramuscular veins (17, 18). Macrophages also can be present (2). A study of seven European cases reported the finding spirochetes in six and a predominance of T cells and macrophages (35, 47). Fiber degeneration and increased expression of major histocompatibility complex class I but not of major histocompatibility complex class II have been reported (35). Attempts to culture spirochetes from muscle biopsy specimens have been unsuccessful (48), but silver staining has revealed the presence of spirochetes (2, 17, 18). Gallium-67 scans have shown intense skeletal muscle uptake in some cases (2, 32). Antibiotic treatment is usually but not always effective (48). Rarely, necrotizing myopathy has been reported (52).

Lyme myositis also has been observed in several experimental animals, including NHPs, rats, mice, and gerbils. It is more common in immunosuppressed animals. Of 35 mice with severe combined immunodeficiency (*scid*) and inoculated with *B. burgdorferi* strain ZS7, 69% had myositis, compared with 0 of 8 IC controls of the same genetic background (36, 51). The inflammation in *scid* mice is mononuclear, interstitial, and perivascular, with associated necrosis of muscle fibers (36, 51). NIH-3 immunodeficient mice persistently infected with *B. burgdorferi* strain 297 also developed advanced interstitial myositis and focal myonecrosis (16). In contrast, myositis was found in only 14% of 14 IC mice of the AKR/N genotype (36), which are susceptible to arthritis. Spirochetes have been observed by nonspecific silver impregnation techniques in skeletal muscle of experimentally infected rats (5, 6) and mice (7). Cadavid et al. reported previously the absence of myositis in immunosuppressed NHPs despite infection by large numbers of spirochetes; in contrast, in cardiac muscle the inflammation was severe despite a lower spirochetal load (11). In another study of IC NHPs inoculated by tick bite with *B. burgdorferi* strain JD1, only one of six animals was found to have myositis (49).

The experiments reported here provide new insights into the aspects of infection and immunity important for skeletal muscle involvement in Lyme borreliosis. We learned that myositis can occur as a complication of infection with some but not all *B. burgdorferi* strains. An effective immune response is likely to eradicate the infection and prevent tissue injury. However, any failure of the immune response may result in persistent low-level infection and chronic inflammation. An important role for antibody and complement deposition in the pathogenesis of neuroborreliosis is suggested by our data. More studies are needed to ascertain the specificity of the antibodies that accumulate in inflamed tissues and to confirm whether persistent low-level infection may be reactivated.

ACKNOWLEDGMENTS

We thank Alan G. Barbour, University of California at Irvine, for assistance with the 16S rRNA TaqMan RT-PCR assay and Bettina Wilske, Max von Pettenkofer-Institut, Ludwig-Maximilians-University, Munich, Germany, for testing of Pbi sera by ELISA and immunoblotting.

These studies were supported by a contract from the National Institute of Allergy and Infectious Diseases, National Institutes of Health (DMID-99-03). D.C. was also supported in part by a grant from the Bureau of Health Professions, Health Resources and Services Administration, to the Hispanic Center of Excellence at UMDNJ—New Jersey Medical School.

REFERENCES

1. **Ahmed, R., B. D. Jamieson, and D. D. Porter.** 1987. Immune therapy of a persistent and disseminated viral infection. J. Virol. **61:**3920–3929.
2. **Atlas, E., S. N. Novak, P. H. Duray, and A. C. Steere.** 1988. Lyme myositis: muscle invasion by Borrelia burgdorferi. Ann. Intern. Med. **109:**245–246.
3. **Barbour, A. G., S. F. Hayes, R. A. Heiland, M. E. Schrumpf, and S. L. Tessier.** 1986. A *Borrelia*-specific monoclonal antibody binds to a flagellar epitope. Infect. Immun. **52:**549–554.
4. **Barbour, A. G., and M. E. Schrumpf.** 1986. Polymorphisms of major surface proteins of Borrelia burgdorferi. Zentbl. Bakteriol. Mikrobiol. Hyg. Ser. A **263:**83–91.
5. **Barthold, S., K. Moody, G. Terwilliger, P. Duray, R. Jacoby, and A. Steere.** 1988. Experimental Lyme arthritis in rats infected with Borrelia burgdorferi. J. Infect. Dis. **157:**842–846.
6. **Barthold, S. W., K. D. Moody, G. A. Terwilliger, R. O. Jacoby, and A. C. Steere.** 1988. An animal model for Lyme arthritis. Ann. N. Y. Acad. Sci. **539:**264–273.
7. **Barthold, S. W., D. H. Persing, A. L. Armstrong, and R. A. Peeples.** 1991. Kinetics of Borrelia burgdorferi dissemination and evolution of disease after intradermal inoculation of mice. Am. J. Pathol. **139:**263–273.
8. **Berger, B. W.** 1984. Erythema chronicum migrans of Lyme disease. Arch. Dermatol. **120:**1017–1021.
9. **Breitner-Ruddock, S., R. Wurzner, J. Schulze, and V. Brade.** 1997. Heterogeneity in the complement-dependent bacteriolysis within the species of Borrelia burgdorferi. Med. Microbiol. Immunol. (Berlin) **185:**253–260.
10. **Burgdorfer, W., A. G. Barbour, S. F. Hayes, J. L. Benach, E. Grunwaldt, and J. P. Davis.** 1982. Lyme disease-a tick-borne spirochetosis? Science **216:**1317–1319.
11. **Cadavid, D., T. O'Neill, H. Schaefer, and A. R. Pachner.** 2000. Localization of Borrelia burgdorferi in the nervous system and other organs in a nonhuman primate model of lyme disease. Lab. Investig. **80:**1043–1054.
12. **Cadavid, D., A. R. Pachner, L. Estanislao, R. Patalapati, and A. G. Barbour.** 2001. Isogenic serotypes of *Borrelia turicatae* show different localization in the brain and skin of mice. Infect. Immun. **69:**3389–3397.
13. **Cadavid, D., P. M. Pennington, T. A. Kerentseva, S. Bergstrom, and A. G. Barbour.** 1997. Immunologic and genetic analyses of VmpA of a neurotropic strain of *Borrelia turicatae*. Infect. Immun. **65:**3352–3360.
14. **Calame, K. L.** 2001. Plasma cells: finding new light at the end of B cell development. Nat. Immunol. **2:**1103–1108.
15. **Centers for Disease Control and Prevention.** 2002. Lyme disease—United States, 2000. Morb. Mortal. Wkly. Rep. **51:**29–31.
16. **Defosse, D. L., P. H. Duray, and R. C. Johnson.** 1992. The NIH-3 immunodeficient mouse is a model for Lyme borreliosis myositis and carditis. Am. J. Pathol. **141:**3–10.
17. **Duray, P. H.** 1989. Clinical pathologic correlations of Lyme disease. Rev Infect. Dis. **11**(Suppl. 6)**:**S1487–S1493.
18. **Duray, P. H.** 1989. Histopathology of clinical phases of human Lyme disease. Rheum. Dis. Clin. North Am. **15:**691–710.
19. **Duray, P. H., and A. C. Steere.** 1986. The spectrum of organ and systems pathology in human Lyme disease. Zentbl. Bakteriol. Mikrobiol. Hyg. Ser. A **263:**169–178.
20. **Ferguson, D. J., J. Huskinson-Mark, F. G. Araujo, and J. S. Remington.** 1994. A morphological study of chronic cerebral toxoplasmosis in mice: comparison of four different strains of Toxoplasma gondii. Parasitol. Res. **80:**493–501.
21. **Fingerle, V., U. Hauser, G. Liegl, B. Petko, V. Preac-Mursic, and B. Wilske.** 1995. Expression of outer surface proteins A and C of *Borrelia burgdorferi* in *Ixodes ricinus*. J. Clin. Microbiol. **33:**1867–1869.
22. **Frey, M., B. Jaulhac, Y. Piemont, L. Marcellin, P. M. Boohs, P. Vautravers, M. Jesel, J. L. Kuntz, H. Monteil, and J. Sibilia.** 1998. Detection of Borrelia burgdorferi DNA in muscle of patients with chronic myalgia related to Lyme disease. Am. J. Med. **104:**591–594.
23. **Gerber, M. A., E. D. Shapiro, G. S. Burke, V. J. Parcells, G. L. Bell, et al.** 1996. Lyme disease in children in southeastern Connecticut. N. Engl. J. Med. **335:**1270–1274.
24. **Hardin, J. A., A. C. Steere, and S. E. Malawista.** 1979. Immune complexes

and the evolution of Lyme arthritis. Dissemination and localization of abnormal C1q binding activity. N. Engl. J. Med. **301:**1358–1363.
25. **Hardin, J. A., L. C. Walker, A. C. Steere, T. C. Trumble, K. S. Tung, R. C. Williams, Jr., S. Ruddy, and S. E. Malawista.** 1979. Circulating immune complexes in Lyme arthritis. Detection by the 125I-C1q binding, C1q solid phase, and Raji cell assays. J. Clin. Investig. **63:**468–477.
26. **Hoffmann, J. C., D. O. Stichtenoth, H. Zeidler, M. Follmann, A. Brandis, G. Stanek, and J. Wollenhaupt.** 1995. Lyme disease in a 74-year-old forest owner with symptoms of dermatomyositis. Arthritis Rheum. **38:**1157–1160.
27. **Horowitz, H. W., K. Sanghera, N. Goldberg, D. Pechman, R. Kamer, P. Duray, and A. Weinstein.** 1994. Dermatomyositis associated with Lyme disease: case report and review of Lyme myositis. Clin. Infect. Dis. **18:**166–171.
28. **Ilowite, N. T.** 1995. Muscle, reticuloendothelial, and late skin manifestations of Lyme disease. Am. J. Med. **98:**63S–68S.
29. **Jauris-Heipke, S., R. Fuchs, M. Motz, V. Preac-Mursic, E. Schwab, E. Soutschek, G. Will, and B. Wilske.** 1993. Genetic heterogenity of the genes coding for the outer surface protein C (OspC) and the flagellin of Borrelia burgdorferi. Med. Microbiol. Immunol. (Berlin) **182:**37–50.
30. **Johnston, Y. E., P. H. Duray, A. C. Steere, M. Kashgarian, J. Buza, S. E. Malawista, and P. W. Askenase.** 1985. Lyme arthritis. Spirochetes found in synovial microangiopathic lesions. Am. J. Pathol. **118:**26–34.
31. **Kalish, R. A., R. F. Kaplan, E. Taylor, L. Jones-Woodward, K. Workman, and A. C. Steere.** 2001. Evaluation of study patients with Lyme disease, 10–20-year follow-up. J. Infect. Dis. **183:**453–460.
32. **Kengen, R. A., M. vd Linde, H. G. Sprenger, and D. A. Piers.** 1989. Scintigraphic evaluation of Lyme disease: gallium-67 imaging of Lyme myositis. Clin. Nucl. Med. **14:**728–729.
33. **Lawrenz, M. B., J. M. Hardham, R. T. Owens, J. Nowakowski, A. C. Steere, G. P. Wormser, and S. J. Norris.** 1999. Human antibody responses to VlsE antigenic variation protein of *Borrelia burgdorferi*. J. Clin. Microbiol. **37:** 3997–4004.
34. **Legoedec, J., P. Gasque, J. F. Jeanne, M. Scotte, and M. Fontaine.** 1997. Complement classical pathway expression by human skeletal myoblasts in vitro. Mol. Immunol. **34:**735–741.
35. **Muller-Felber, W., C. D. Reimers, J. de Koning, P. Fischer, A. Pilz, and D. E. Pongratz.** 1993. Myositis in Lyme borreliosis: an immunohistochemical study of seven patients. J. Neurol. Sci. **118:**207–212.
36. **Museteanu, C., U. E. Schaible, T. Stehle, M. D. Kramer, and M. M. Simon.** 1991. Myositis in mice inoculated with Borrelia burgdorferi. Am. J. Pathol. **139:**1267–1271.
37. **Nepomuceno, R. R., and A. J. Tenner.** 1998. C1qRP, the C1q receptor that enhances phagocytosis, is detected specifically in human cells of myeloid lineage, endothelial cells, and platelets. J. Immunol. **160:**1929–1935.
38. **Pachner, A. R., J. Basta, E. Delaney, and D. Hulinska.** 1995. Localization of Borrelia burgdorferi in murine Lyme borreliosis by electron microscopy. Am. J. Trop. Med. Hyg. **52:**128–133.
39. **Pachner, A. R., and D. Cadavid.** 2002. Lyme neuroborreliosis. *In* R. C. Griggs and R. J. Joynt (ed.), Clinical neurology on CD ROM. Lippincott-Raven, Philadelphia, Pa.
40. **Pachner, A. R., D. Cadavid, G. Shu, D. Dail, S. Pachner, E. Hodzic, and S. W. Barthold.** 2001. Central and peripheral nervous system infection, immunity, and inflammation in the NHP model of Lyme borreliosis. Ann. Neurol. **50:**330–338.
41. **Pachner, A. R., E. Delaney, and T. O'Neill.** 1995. Neuroborreliosis in the nonhuman primate: Borrelia burgdorferi persists in the central nervous system. Ann. Neurol. **38:**667–669.
42. **Pachner, A. R., E. Delaney, T. O'Neill, and E. Major.** 1995. Inoculation of nonhuman primates with the N40 strain of Borrelia burgdorferi leads to a model of Lyme neuroborreliosis faithful to the human disease. Neurology **45:**165–172.
43. **Pachner, A. R., E. Delaney, W. F. Zhang, T. O'Neill, E. Major, A. B. Frey, and E. Davidson.** 1999. Protection from Lyme neuroborreliosis in nonhuman primates with a multiantigenic vaccine. Clin. Immunol. **91:**310–313.
44. **Pachner, A. R., H. Gelderblom, and D. Cadavid.** 2001. The rhesus model of Lyme neuroborreliosis. Immunol. Rev. **183:**186–204.
45. **Pachner, A. R., H. Schaefer, K. Amemiya, D. Cadavid, W. F. Zhang, K. Reddy, and T. O'Neill.** 1998. Pathogenesis of neuroborreliosis—lessons from a monkey model. Wien Klin. Wochenschr. **110:**870–873.
46. **Philipp, M. T., M. K. Aydintug, R. P. Bohm, Jr., F. B. Cogswell, V. A. Dennis, H. N. Lanners, R. C. Lowrie, Jr., E. D. Roberts, M. D. Conway, M. Karacorlu, et al.** 1993. Early and early disseminated phases of Lyme disease in the rhesus monkey: a model for infection in humans. Infect. Immun. **61:**3047–3059.
47. **Reimers, C. D., J. de Koning, U. Neubert, V. Preac-Mursic, J. G. Koster, W. Muller-Felber, D. E. Pongratz, and P. H. Duray.** 1993. Borrelia burgdorferi myositis: report of eight patients. J. Neurol. **240:**278–283.
48. **Reimers, C. D., D. E. Pongratz, U. Neubert, A. Pilz, G. Hubner, M. Naegele, B. Wilske, P. H. Duray, and J. de Koning.** 1989. Myositis caused by Borrelia burgdorferi: report of four cases. J. Neurol. Sci. **91:**215–226.
49. **Roberts, E. D., R. P. Bohm, Jr., F. B. Cogswell, H. N. Lanners, R. C. Lowrie, Jr., L. Povinelli, J. Piesman, and M. T. Philipp.** 1995. Chronic Lyme disease in the rhesus monkey. Lab. Investig. **72:**146–160.
50. **Roehrig, J. T., J. Piesman, A. R. Hunt, M. G. Keen, C. M. Happ, and B. J. Johnson.** 1992. The hamster immune response to tick-transmitted Borrelia burgdorferi differs from the response to needle-inoculated, cultured organisms. J. Immunol. **149:**3648–3653.
51. **Schaible, U. E., R. Wallich, M. D. Kramer, C. Museteanu, and M. M. Simon.** 1991. A mouse model for Borrelia burgdorferi infection: pathogenesis, immune response and protection. Behring Inst. Mitt. **88:**59–67.
52. **Schoenen, J., J. Sianard-Gainko, M. Carpentier, and M. Reznik.** 1989. Myositis during Borrelia burgdorferi infection (Lyme disease). J. Neurol. Neurosurg. Psychiatry **52:**1002–1005.
53. **Schoenfeld, R., B. Araneo, Y. Ma, L. M. Yang, and J. J. Weis.** 1992. Demonstration of a B-lymphocyte mitogen produced by the Lyme disease pathogen, *Borrelia burgdorferi*. Infect. Immun. **60:**455–464.
54. **Schweizer, A., J. Rohrer, J. W. Slot, H. J. Geuze, and S. Kornfeld.** 1995. Reassessment of the subcellular localization of p63. J. Cell Sci. **108:**2477–2485.
55. **Sell, S., and E. Max.** 2001. Immunology, immunopathology, and immunity, 6th ed., p. 19–20. ASM Press, Washington, D.C.
56. **Steere, A. C.** 2001. Lyme disease. N. Engl. J. Med. **345:**115–125.
57. **Steere, A. C.** 1995. Musculoskeletal manifestations of Lyme disease. Am. J. Med. **98:**44S–48S.
58. **Steere, A. C.** 1988. Pathogenesis of Lyme arthritis: implications for rheumatic disease. Ann. N. Y. Acad. Sci. **539:**87–92.
59. **Steere, A. C., N. H. Bartenhagen, J. E. Craft, G. J. Hutchinson, J. H. Newman, D. W. Rahn, L. H. Sigal, P. N. Spieler, K. S. Stenn, and S. E. Malawista.** 1983. The early clinical manifestations of Lyme disease. Ann. Intern. Med. **99:**76–82.
60. **Steere, A. C., A. R. Pachner, and S. E. Malawista.** 1983. Neurologic abnormalities of Lyme disease: successful treatment with high-dose intravenous penicillin. Ann. Intern. Med. **99:**767–772.
61. **Turley, H., A. Banham, K. Pulford, and K. Gatter.** 1998. B-cell bind panel: antibodies recognizing the human P63 protein, p. 245–248. *In* T. Kishimoto, et al. (ed.), Leucocyte typing VI: white cell differentiation antigens. Garland Publishing Inc., New York, N.Y.
62. **van den Berg, R. H., M. C. Faber-Krol, R. B. Sim, and M. R. Daha.** 1998. The first subcomponent of complement, C1q, triggers the production of IL-8, IL-6, and monocyte chemoattractant peptide-1 by human umbilical vein endothelial cells. J. Immunol. **161:**6924–6930.
63. **Wilske, B., U. Hauser, G. Lehnert, and S. Jauris-Heipke.** 1998. Genospecies and their influence on immunoblot results. Wien Klin. Wochenschr. **110:** 882–885.
64. **Yasojima, K., C. Schwab, E. G. McGeer, and P. L. McGeer.** 1998. Human heart generates complement proteins that are upregulated and activated after myocardial infarction. Circ. Res. **83:**860–869.
65. **Zeidner, N., M. L. Mbow, M. Dolan, R. Massung, E. Baca, and J. Piesman.** 1997. Effects of *Ixodes scapularis* and *Borrelia burgdorferi* on modulation of the host immune response: induction of a Th2 cytokine response in Lyme disease-susceptible (C3H/HeJ) mice but not in disease-resistant (BALB/c) mice. Infect. Immun. **65:**3100–3106.
66. **Zeidner, N. S., M. S. Nuncio, B. S. Schneider, L. Gern, J. Piesman, O. Brandao, and A. R. Filipe.** 2001. A Portuguese isolate of Borrelia lusitaniae induces disease in C3H/HeN mice. J. Med. Microbiol. **50:**1055–1060.
67. **Zumstein, G., R. Fuchs, A. Hofmann, V. Preac-Mursic, E. Soutschek, and B. Wilske.** 1992. Genetic polymorphism of the gene encoding the outer surface protein A (OspA) of Borrelia burgdorferi. Med. Microbiol. Immunol. **181:** 57–70.

Editor: D. L. Burns